How to cite: *Angew. Chem. Int. Ed.* **2024**, *63*, e202314143
doi.org/10.1002/anie.202314143

Drug Delivery **Hot Paper**

Macrocyclic Dual-Locked "Turn-On" Drug for Selective and Traceless Release in Cancer Cells

Dominik Schauenburg, Bingjie Gao, Léa N. C. Rochet, Darijan Schüler, Jaime A. S. Coelho, David Y. W. Ng, Vijay Chudasama, Seah Ling Kuan, and Tanja Weil**

Abstract: Drug safety and efficacy due to premature release into the bloodstream and poor biodistribution remains a problem despite seminal advances in this area. To circumvent these limitations, we report drug cyclization based on dynamic covalent linkages to devise a dual lock for the small-molecule anticancer drug, camptothecin (CPT). Drug activity is "locked" within the cyclic structure by the redox responsive disulfide and pH-responsive boronic acid-salicylhydroxamate and turns on only in the presence of acidic pH, reactive oxygen species and glutathione through traceless release. Notably, the dual-responsive CPT is more active (100-fold) than the non-cleavable (permanently closed) analogue. We further include a bioorthogonal handle in the backbone for functionalization to generate cyclic-locked, cell-targeting peptide- and protein-CPTs, for targeted delivery of the drug and traceless release in triple negative metastatic breast cancer cells to inhibit cell growth at low nanomolar concentrations.

[*] Dr. D. Schauenburg, B. Gao, D. Schüler, Dr. D. Y. W. Ng, Dr. S. L. Kuan, Prof. Dr. T. Weil
Synthesis of Macromolecules
Max Planck Institute for Polymer Research
55128 Mainz, Germany
E-mail: kuan@mpip-mainz.mpg.de
weil@mpip-mainz.mpg.de

L. N. C. Rochet, Prof. Dr. V. Chudasama
Department of Chemistry
University College London
London WC1H 0AJ, UK

Dr. J. A. S. Coelho
Centro de Química Estrutural
Institute of Molecular Sciences
Faculty of Sciences
University of Lisbon
1749-016 Lisbon, Portugal

Dr. S. L. Kuan, Prof. Dr. T. Weil
Institute of Inorganic Chemistry I
Ulm University
89081 Ulm, Germany

Introduction

Chemotherapy is one of the mainstream treatments to combat cancer, but the safety and efficacy limitations of anticancer drugs persist due to their often indiscriminate biodistribution in healthy and tumor tissue.[1] To improve the efficacy of existing small-molecule anticancer drugs, targeted therapeutics have been developed that combine a small-molecule drug with a cell recognition moiety that binds exclusively to and penetrates cancer cells.[2] Examples include peptide- or antibody-drug conjugates and targeted nanoparticle delivery systems.[3,4] Peptide- and antibody-drug conjugates offer certain advantages over targeted nanoparticle systems, as the nanoparticle can bind to plasma proteins that shield the targeting groups and thus compromise the targeting effect in vivo.[5] Besides targeting, stability in blood plasma without burst or premature release of cargo in low glutathione (GSH) concentrations (μM) through disulfide exchange reactions or in acidic extracellular tumor microenvironments (TME) of malignant tumors (extracellular pH 6.5–6.9) are required to reduce off-target toxicity.[6–9] Additionally, controlled drug release from the targeting group within tumor cells or a nanoparticle formulation should, ideally, be quantitative for high therapeutic efficacy. However, to date, there are limited linker chemistries that fulfill these criteria. Therefore, new strategies are urgently needed to furnish an anticancer drug that 1) prevents premature release in blood plasma; 2) exhibits low drug toxicity outside tumor microenvironments or cancer cells; 3) possesses the availability of a targeting group to bind to cell surface receptors expressed on cancer cells with high affinity; 4) enables controlled quantitative traceless drug release in cancer cells to convert the inactive drug into its active form.

Cyclic peptide or peptoid structures in Nature, for example, in peptide hormones[10] or snake venom,[11] have inspired the design of drug candidates.[12,13]

Besides their improved stability and bioavailability,[14] one of the eminent features of cyclization in Nature is activity control. Bioactivity can be influenced by a conformational switch from the cyclic (closed/locked) to the linear (open) form, suggesting that embedding small-molecule drugs within a cyclic and cleavable "lock" would be a viable approach to reduce premature release by selective drug activation in cancer cells.[14] However, it is synthetically challenging to combine a small-molecule drug, a targeting group and stimuli-responsiveness within a cyclic structure, with limited examples in literature.[15,16] Moreover, it is even

more difficult to introduce functionalities that respond to two independent stimuli using the classical head-to-tail cyclization approach (Figure 1). We recently reported the combination of redox responsive disulfides and pH responsive catechol – boronic acids (BAs) containing interlocked peptide linkers that display dual-stimuli-responsiveness, with improved stability and controlled disassembly in tumor cells.[17] Therefore, this strategy could offer a broadly applicable approach to enable directionality to form a cyclic-locked, dual stimuli-responsive drug for controlled release combined with a cell targeting group for biorecognition (Figure 1).

Boronic acids (BAs) can undergo pH-reversible coordination to diols and salicylhydroxamates (SHAs), as well as provide traceless release in the presence of high hydrogen peroxide (H_2O_2) concentrations of in cancer cells to afford the alcohol group in cargo drugs.[18] We selected SHA, which offers several advantages over catechol groups, with better binding affinity to BAs (μM versus mM) to afford stable conjugates at low concentrations (μM), while being rapidly and quantitatively cleavable at acidic pH (Figure 1).[19–21] Under physiological pH in healthy tissue, the structure remains in its "closed" form but opens in the acidic environment of subcellular compartments.[22] Additionally, BAs offer more chemical innovation space for pharmaceuticals as they are non-toxic, as exemplified by several marketed drugs with boronic acid groups such as Eucrisa™ or Vabomere™, among others, which are used in clinical trials.[18,23] Furthermore, due to the elevated content of reactive oxygen species (ROS) present in cancer cells such as H_2O_2,[24] boric acid "masked" alcohol functional groups can be restored by oxidation in cancer cells in a traceless fashion (Figure 1). A disulfide linkage is introduced as a second chemical lock to control the release within cytosolic compartments and prevent cleavege in the acidic extracellular space within the TME.[25–27] Disulfides remain stable over several pH units but they can undergo self-immolative intracellular reduction in tumor cells in the presence of high intracellular GSH concentration.[28–30] This restores the activity of the drug cargo, which may be an advantage over conventional disulfide linkers that result in loss of drug activity due to the formation of less active glutathione-drug conjugates.[31] However, premature burst release of disulfide containing pro-drugs in the blood circulation still represents a concern that could potentially be prevented in combination with an intramolecular SHA-BA lock that is stable at neutral pH and in the absence of high concentrations of reactive oxygen species.[32–34]

We choose the pentacyclic natural product, camptothecin (CPT), as the drug lead structure (Scheme 1A).[35,36] CPT binds to nuclear enzyme DNA topoisomerase I (TOP1) and DNA complexes, which ultimately leads to apoptosis.[37,38] Different analogues of the topoisomerase I inhibitor are FDA approved, highly potent (IC_{50} low nM), and they have been widely applied for treatment of leukemia, lung cancer, breast cancer, among others.[39–41] In addition, we introduced a bioorthogonal reactive handle for post-functionalization of the macrocyclic drug, where the targeting moiety is linked via a stable covalent linkage. In this way, we could generate cell-targeting peptide-macrocyclic and protein-macrocyclic CPTs for traceless drug release in triple negative metastatic breast cancer cells to inhibit cell growth. We envision that

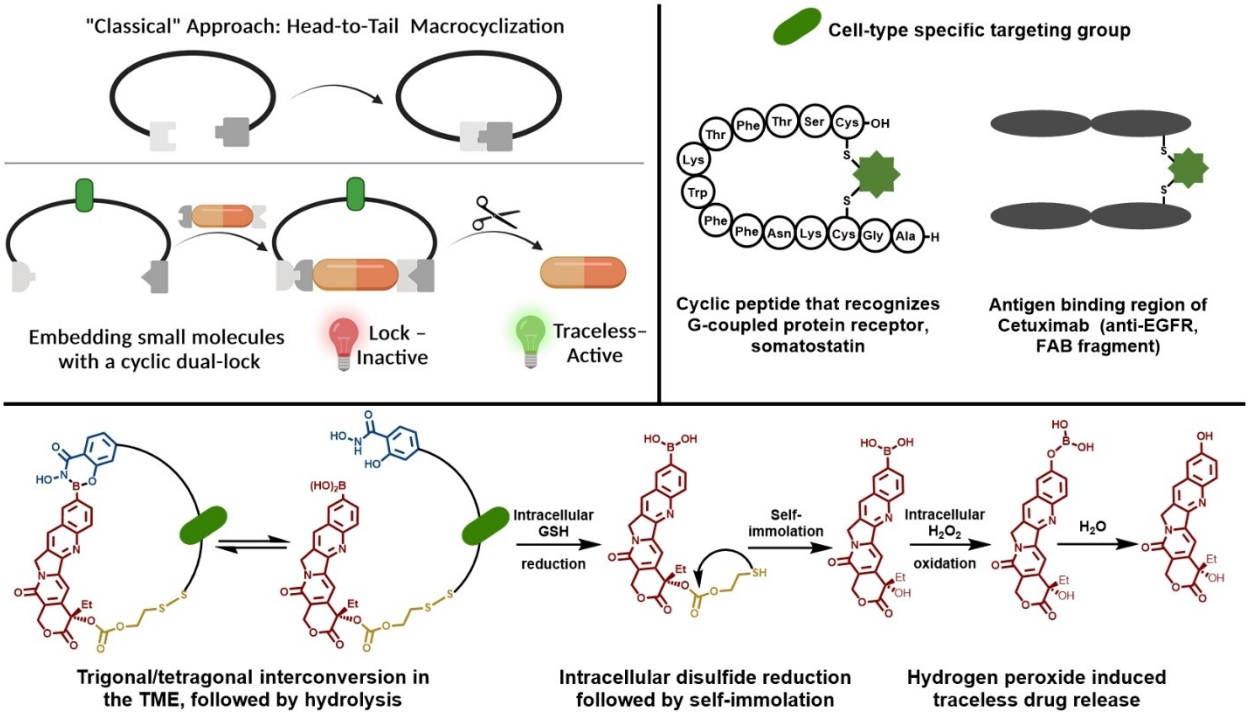

Figure 1. Conceptual overview of the "classical approach" for macrocyclization, a cyclic dual-locked CPT that allows selective and traceless release in cancer cells, and a possible reaction Scheme for sequential cleavage and traceless CPT release.

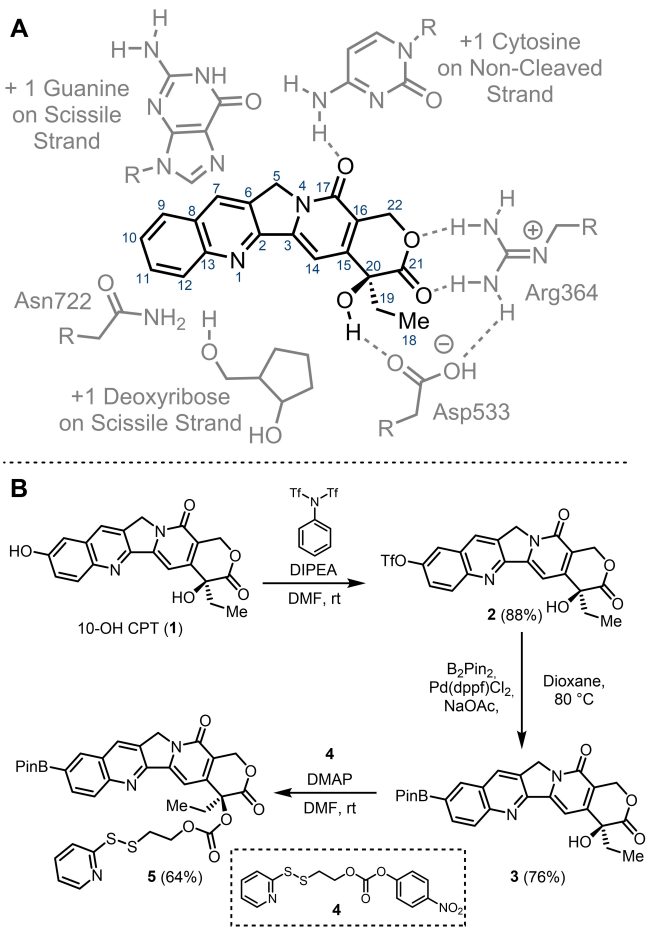

Scheme 1. Proposed CPT binding and functionalization. A) Key hydrogen bonds and ring-stacking interactions between the human topoisomerase I–DNA covalent complex and CPT in the proposed CPT binding mode. The atomic nomenclature for CPT is also indicated.[37] B) Synthesis of key intermediate 10-pinacolborane (BPin) CPT pyridyl disulfide (**5**, Supporting Information page 6–7). DIPEA = *N*,*N*-diisopropylethylamine, DMAP = 4-dimethylaminopyridine, DMF = *N*,*N*-dimethylformamide, dppf = 1,1′-bis(diphenylphosphanyl)ferrocene, Pin = pinacolato, Tf = trifluoromethanesulfonyl.

targeted dual-stimuli-responsive macrocyclic chemotherapeutics can be positioned as an efficient strategy to generate drugs without premature release into the bloodstream nor in the acidic TME revealing selective and traceless drug release in the chemical environment relevant for cancer cells.

Results and Discussion

To prepare a dual-responsive cyclic CPT analogue, we introduced a boronic acid moiety on the quinoline ring (Scheme 1B), as previously shown for the prodrug of SN-38.[42] The alcohol of the α-hydroxy lactone was modified with a self-immolative disulfide linker.[43,44] In this way, traceless CPT release could be achieved, which is essential for bioactivity. We started the synthesis with the trifluoromethanesulfonation of commercially available 10-OH CPT (**1**) using *N*-phenylbis(trifluoromethanesulfonimide) followed by palladium catalyzed Miyaura-borylation resulting in 10-BPin CPT (**3**, see Scheme 1B). The alcohol functionality on the stereocenter (C20) of **3** was transformed to the corresponding carbonate, using the activated disulfide **4** in the presence of DMAP, providing compound **5** in an overall yield of 42 % (over three steps).

With 10-BPin-CPT pyridyl disulfide (**5**) in hand, we performed disulfide exchange with *N*-acetylcysteine amide. The pinacolborane conveniently hydrolyzed during HPLC purification, yielding the unprotected boronic acid **7** (Figure 2A). A non-cleavable analogue consisting of a cysteine thioether was synthesized as a control for subsequent investigation (**8**, Figure 2A). The prepared CPT derivatives were subjected to cellular growth assays using MDA-MB-231 triple-negative breast cancer cells. Cellular growth was monitored over 110 h using an Incucyte® Live-Cell Analysis System, which is able to capture high-resolution bright field images and record data in real-time, directly in the incubator (Figure 2B, experimental details in Supporting Information page 64).

As expected, 10-OH CPT (**1**) displayed high inhibition in the proliferation assay. At a concentration of 50 nM, no significant cell growth was observed. The IC_{50} value was

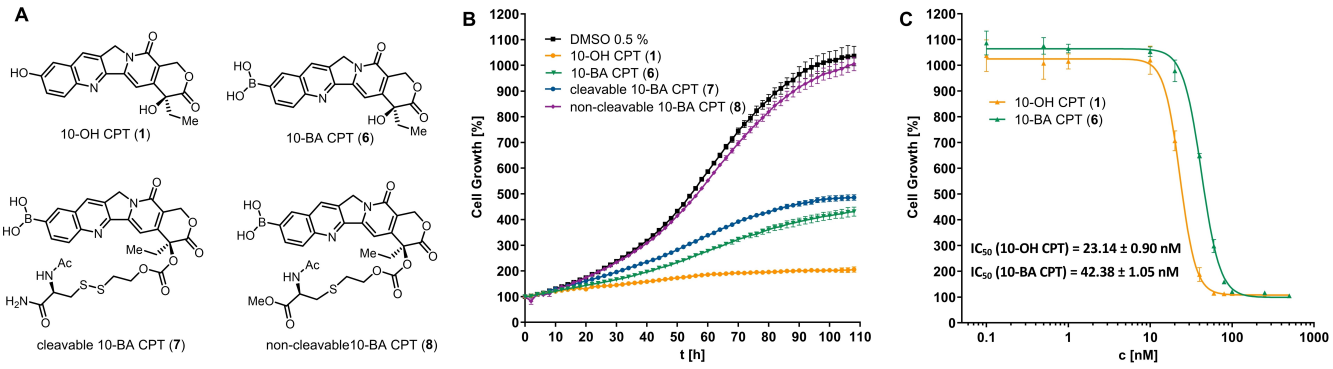

Figure 2. A) Structures of CPT derivatives subjected to the cell proliferation assay. B) Cellular growth of MDA-MB-231 cells by treatment with different CPT derivatives at 50 nM concentration. C) Determination of IC_{50} values of 10-OH CPT (**1**) and 10-BA-CPT (**6**) in MDA-MB-231 cells. DMSO = dimethyl sulfoxide.

determined to be 23.1 ± 0.9 nM. Boronic acid modified CPT **6** showed lower activity with a twofold higher IC_{50} value of 42.4 ± 1.1 nM. In contrast, the non-cleavable analogue **8** resulted in almost no difference in cell growth inhibition when compared to the DMSO control. The disulfide containing, self-immolative analogue **7** was as potent as 10-BA CPT at a concentration of 50 nM suggesting that efficient disulfide reduction took place under these conditions.

Based on these results, our next step was to embed the drug in a cyclic structure to achieve selective, dual-responsive and traceless release in the unique intracellular cancer environment.

Design and Synthesis of Cyclic CPT Derivatives

To enable cell-targeted dual-stimuli responsive delivery and release of CPTs, a trifunctional linker was designed. The water-soluble linker containing SHA, a thiol, an appropriate number of Fmoc-8-amino-3,6-dioxaoctanoic acid (Fmoc-AEEAc-OH) linkers in between the SHA and thiol to form the cyclic structure, and a bioorthogonal chemical handle for further conjugation (azide or DBCO), were conveniently conjugated on the solid support, with only one step-purification required by HPLC (Figure 3A).

The length of the linker was predicted by molecular modeling to determine the number of AEEAc-OH spacers necessary to facilitate intramolecular cyclization of the SHA to the BA (Figure 3E). The theoretical feasibility of the intramolecular cyclization was assessed by analyzing the macrocyclization equilibria, assuming a thermodynamically controlled process. To determine the relative Gibbs free energies of cyclic and open-chain structures for SHA-$(AEEAc)_n$-Cys(CPT-BA)-NHFmoc ($n = 0$, 1, 4), density functional theory (DFT) calculations were performed. As the planarity of the SHA and CPT-BA could hinder intramolecular cyclization, a longer linker (e.g., 4 AEEAc groups) would presumably enhance the efficiency of macrocyclization. Indeed, DFT calculations showed that the energy difference between the open and closed structures for SHA-$(AEEAc)_4$-Cys(CPT-BA)-NHFmoc is 8.6 kcal mol^{-1}, whereas for SHA-$(AEEAc)_1$-Cys(CPT-BA)-NHFmoc is 15.4 kcal mol^{-1}, which is in agreement with the assumption.

Therefore, we proceeded to prepare the linkers **9** and **10**. Besides "standard" Fmoc-SPPS, we utilized copper(I)-catalyzed azide-alkyne cycloaddition (CuAAC), palladium(0)-catalyzed alloc deprotection, acid mediated monomethoxytrityl (MMT) deprotection and thio-ether bond formation, directly on resin to afford compound **9** and **10** (Figure 3A–B). After acidic deprotection, disulfide exchange of **5** to the Cys-side chain of the respective linker was performed to give **11** or **12** in the "open" conformation (Figure 3B). The successful switching between intramolecular cyclization ("closed") and linear ("opened") structure was characterized and confirmed by high resolution electrospray ionization (ESI) (Figure 3C and 3D), showing a change in the *m/z* of 36 Da. This change in m/z is due to the release of two water molecules after the condensation reaction, which corroborates with the calculated exact mass of the respective structures.

Cleavage and Stability under Biologically Relevant Conditions of CPT Derivatives

Cancer cells are known to exhibit higher concentrations of reactive oxygen species such as hydrogen peroxide,[24] elevated levels of glutathione (GSH)[45] and often an acidic extracellular matrix. Thus, the cleavage and stability of various CPT derivatives under biologically relevant conditions were determined. A time course for the cleavage of the disulfide bond in **7** by glutathione to induce self-immolative release of CPT-boronic acid (10-BA CPT, **6**) was conducted in reducing conditions (SI-Figure S43–S45). The glutathione concentration in cancer cells is abnormally high (up to 10 mM) compared to the extracellular matrix (10 μM), in blood (up to 20 μM) or normal cells (1–2 mM).[22,28,29,46,47] To test for cleavage/stability towards GSH relevant for intracellular conditions in cancer cells, compound **7** (50 μM) was dissolved in ammonium bicarbonate buffer (50 mM, pH 7.4 or 6.5) containing 10 mM GSH, 1 mM glutathione disulfide (GSSG) (SI-Figures 43 and 44). The stability was monitored by high-performance liquid chromatography (HPLC) or LC–MS and showed clean conversion of the disulfide to 10-BA CPT at both pH values (SI-Figures 43 and 44). At medium GSH concentration (100 μM), compound **7** remained stable for up to three days (SI-Figure S45).

H_2O_2 is often present at higher concentrations in cancer cells (10–50 μM), [48–52] where fast oxidation of boronic acids has been reported.[21,53] To verify this, we tested the oxidation of compound **7**, which contains a boronic acid group and a disulfide linker, in the presence of 50 μM of H_2O_2 at pH 7.4. The boronic acid group in compound **7** undergoes a traceless conversion to the alcohol, while the disulfide bond remained intact, as observed in the LC–MS (SI-Figure S46).

It is known that CPT has a high plasma protein binding (> 80 % in many cases), which limits its bioavailability.[54] Thus, a dual locked analogue without fluorescent dye (**11**) was incubated in human serum, as well as in cell lysates and monitored using LC–MS. Just a slight decrease in the amount of **11** after 4 h incubation time was observed. It remains stable up to 24 h (ca. 10 % for cell lysates and approximately 20–30 % for human serum, SI-Figures S47 and S48). Also, we did not observe exchange reactions with thiol-containing lysate or serum components, which is in line with previous studies, where disulfide exchange was reduced in combination with stabilizing boronic acid complexes.[17] Furthermore, CPT has a low water solubility at physiological pH (6–15 μM), whereas the cyclic CPT **12** could be dissolved in 100 μM without any problems.[55]

To explore the effect of a dual-locked cyclic CPT versus singly caged variants in biologically relevant conditions, we performed Förster Resonance Energy Transfer (FRET) studies. Intramolecular FRET occurs at dilute conditions if a

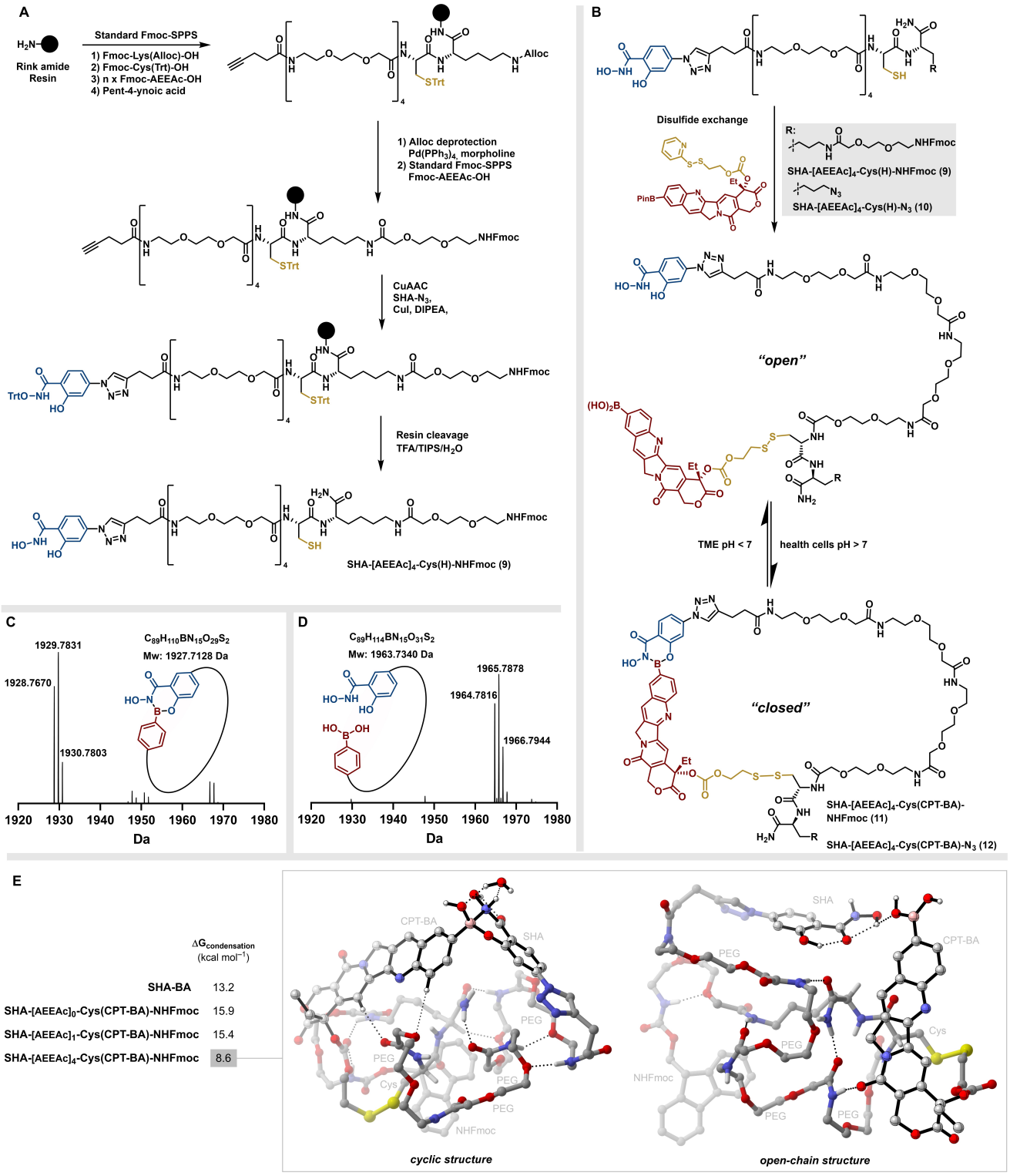

Figure 3. Synthesis and characterization of dual-stimuli-responsive CPT analogues **11** and **12**. A) Preparation of the trifunctional linker by Fmoc-SPPS ("standard Fmoc-SPPS" refers to: Fmoc-deprotection using 20 vol% piperidine in DMF, preactivation of the AA with hexafluorophosphate azabenzotriazole tetramethyl uranium/*N*,*N*-diisopropylethylamine (HATU/DIPEA), *N*,*N*′-diisopropylcarbodiimide/ethyl cyanohydroxyiminoacetate (DIC/Oxyma, for Cys) and capping using 20 vol% of acetic anhydride in DMF, respectively. B) "Loading" of CPT analogue (**5**) by disulfide exchange, structure of the "opened" and the "closed" form (isolated yield of **11**: 30%, of **12**: 28%, from initial SPPS loading). Intramolecular cyclization of CPT. C) High-resolution electrospray ionization mass spectrometry (HR-ESI-MS) analysis of dual-stimuli responsive CPT (**11**) in ammonium acetate buffer at pH 7.4, "cyclic" structure (calcd for $C_{89}H_{110}BN_{15}O_{29}S_2$: 1927.7128 Da); D) HR-ESI-MS analysis of dual-stimuli-responsive CPT (**11**) in ammonium acetate buffer at pH 6.5, "open" structure (calcd for $C_{89}H_{114}BN_{15}O_{31}S_2$: 1963.7340 Da). E) Molecular modeling (some hydrogen atoms are omitted for clarity) and theoretical evaluation of the macrocyclization process with calculated $\Delta G_{condensation}$ values. DFT calculations performed at M06-2X/Def2-TZVPP/SMD(water)//B3LYP/6-31G(d) level of theory.

fluorescent donor-acceptor pair with overlapping emission and absorption spectra are in close proximity,[56] which give optical information whether the cleavage of the cyclic linker took place. To demonstrate the release of CPT, the intrinsic fluorescence of CPT was utilized as a FRET donor dye and *N*-ethylamide-4-dimethyl-1,8-naphthalimide was installed on a Lys-side chain of the linker as an acceptor dye[57] in the dual-responsive CPT **13** and linear mono-responsive CPTs **14** and **15** (Figure 4A–D) were studied as well. As a control, the fluorescence of 10-BA CPT (**6**) was first evaluated at pH 7.4 and 6.5 (25 μM in PB buffer containing 10 % DMSO at rt), as well as in the presence and absence of GSH (10 mM). A strong fluorescence band with a maximum at 428 nm under excitation at 385 nm was found (Figure S55 and S56). For subsequent experiments, we compared the fluorescence intensity at 428 nm.

Fluorescence quenching was observed for the singly caged, mono-responsive CPT with a disulfide bond (**14**, Figure 4B, E) at pH 7.4 (PB). After addition of GSH, a significant increase in fluorescence intensity (ca. 50-fold) was observed, indicating cleavage of the disulfide and release of the CPT. Quenching occurred for the singly caged, pH-responsive BA-SHA CPT conjugate **15** at pH 7.4 (Figure 4C,E). A clear increase in fluorescence intensity (ca. 10-fold) was observed at pH 6.5, suggesting the release of the CPT. On the other hand, the fluorescence signal of the dual-stimuli-responsive CPT **13** (Figure 4A, E) indicated that this compound was much more stable in the presence of a single stimulus. Quenching occurred at pH 7.4 and 6.5, as well as after adding GSH at pH 7.4, which clearly demonstrated that CPT cannot be released in the cyclic form by a single stimulus only. However, a strong fluorescence signal was detected at pH 6.5 and in the presence of GSH (Figure 4E). Therefore, both chemical triggers (GSH and low pH) were required to unlock the double hinges to release the CPT from the cyclic structure in **13**.

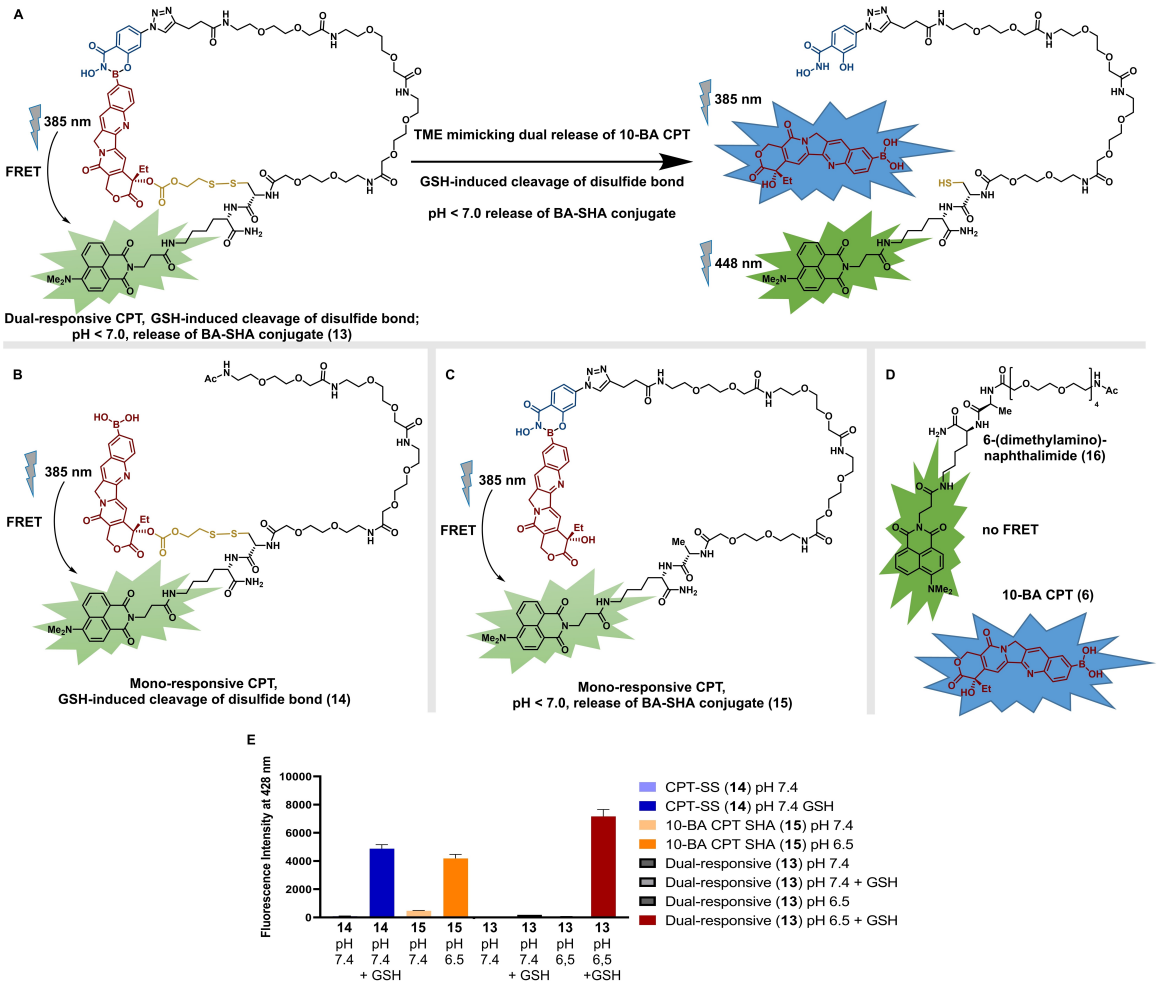

Figure 4. Förster resonance energy transfer (FRET) of CPT derivatives. Studies were carried out with 25 μM of the CPT derivative or control in PB buffer containing 10 % DMSO at room temperature at different pH values and reductive conditions (10 mM GSH). Full spectra are available in Figures S55 and S56. A) GSH-induced cleavage of the disulfide bond and concomitant release at pH 6.5 of BA-SHA in dual-responsive CPT conjugate **13**. B) Mono-responsive CPT **14** shows GSH-induced cleavage of the disulfide bond already at neutral pH. C) Mono-responsive CPT **15** reveals release at pH 6.5. D) 4-Dimethylamino-1,8-naphthalimide derivative **16** and 10-BA CPT (**6**) as controls. E) Comparison of the fluorescence intensity for CPT derivatives and stimuli-responsive release at different pH values (6.5 or 7.4) and reductive conditions (10 mM GSH). Emission intensity was measured at 428 nm with an excitation wavelength of 385 nm.

Taken together, the results underline the unique features of the dual-responsive macrocyclic structure compared to the corresponding singly caged derivatives. We provide evidence that premature release of the free CPT does not occur in human serum, cell lysate and acidic extracellular environments such as those of glycolytic tumors. The compound can be unlocked only with the two stimuli to release the active drug in the chemical environment found in cancer cells.

Synthesis of Cell-Targeting Macrocyclic Dual-Locked CPT

To further improve selectivity of the macrocyclic CPT drug, we demonstrated the feasibility of post-functionalization of the newly designed cyclic CPT drug to implement targeting through binding to overexpressed surface receptors on cancer cells. A series of CPT analogues with bioorthogonal handle for strain-promoted copper-free azide-alkyne cycloaddition (SPAAC) were designed (Figure 5). Besides the dual responsive CPT-azide (**12**), a benzyl thio-ether, similar in size to the salicylhydroxamate (SHA) was introduced at the 10-position, as a "non-cleavable – open" analogue (compound **17**, Figure 5A, Supporting Information pages 24–25). A "non-cleavable – cyclic" CPT derivative **18** was prepared by cyclization through CuAAc to propargyl glycine side chain (Figure 5A, Supporting Information pages 29–30). The compounds **12**, **17** and **18** were purified using HPLC and isolated in 28, 63, 58 % yield, respectively. The compounds were characterized using LC–MS (SI-Figure S14, S21, S26).

Two different cancer cell-targeting entities were attached by SPAAC. First, the cyclic growth hormone peptide somatostatin, which binds to G-coupled protein receptors (SSTR), known to be overexpressed in triple negative MDA-MB-231 cancer cells was chosen.[58,59] Disulfide re-bridging of SST with a DBCO or azide linker yielded SST–DBCO/azide **19** and **20** (SI pages 31–32) in 47 % and 42 % yield, respectively. SST conjugated CPTs **23**–**25** (Figure 6A, Supporting Information pages 33–37) were prepared by SPAAC of **12**, **17** or **18** to its corresponding SST analogue (Figure 5). Next, we conjugated azide or bicyclononyne (BCN)-modified Cetuximab antibody fragment (FAB, MW ca. 50 kDa) with cleavable or non-cleavable CPT derivative to afford dual responsive CPT-FAB **26** and non-cleavable CPT-FAB **27** (Figure 6B, Supporting Information pages 39–45). The Cetuximab FAB is often employed as EGFR targeting group.[60,61] Full chemical structures of the CPT-SST/FAB compounds are given in the Supporting Information (pages 33–37 and 39).

In Vitro Studies of Macrocyclic Dual-Locked CPT in Cancer Cells

Next, we investigated the binding of the targeted-cyclic CPT to cell lines with the respective receptors and whether the dual-stimuli-responsive CPT derivatives could be activated in cancer cells, as compared to non-cleavable CPTs that retain their cyclic structure in the TME (extra- and intracellular).

Radioligand binding assays of dual-responsive CPT-SST (**23**) showed binding to the somatostatin receptors of human recombinant CHO-K1 cells with low nanomolar IC_{50} value (3.5 nM, SI-Figure 58), suggesting that modified SST retained its receptor binding affinity expressed on the CHO-K1 cells. Thereafter, we incubated MDA-MB-231 cells with

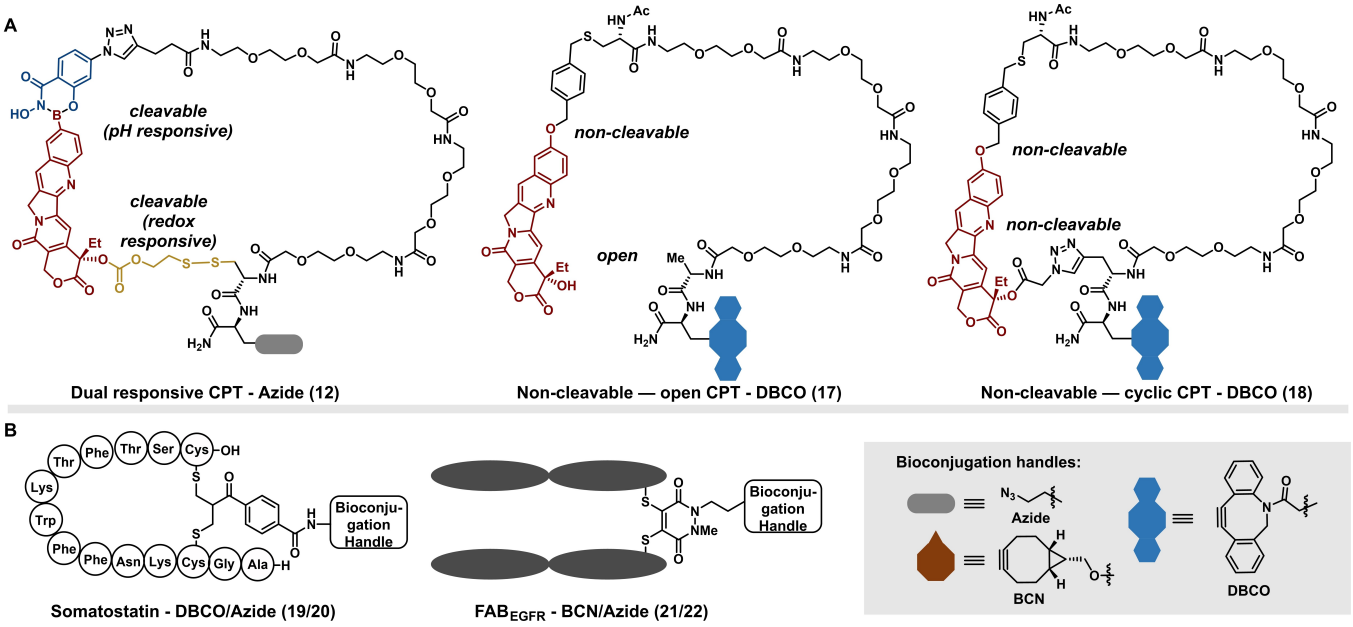

Figure 5. Prepared CPT derivatives and tumor-selective targeting moieties. A) Cleavable and non-cleavable CPT analogues with bioorthogonal handles for further functionalization. B) Cell-targeting entities, namely, somatostatin and FAB$_{EGFR}$ functionalized with the corresponding bioconjugation handles for reaction with CPT derivatives in (A). Inset shows the structure of the various bioorthogonal handles used.

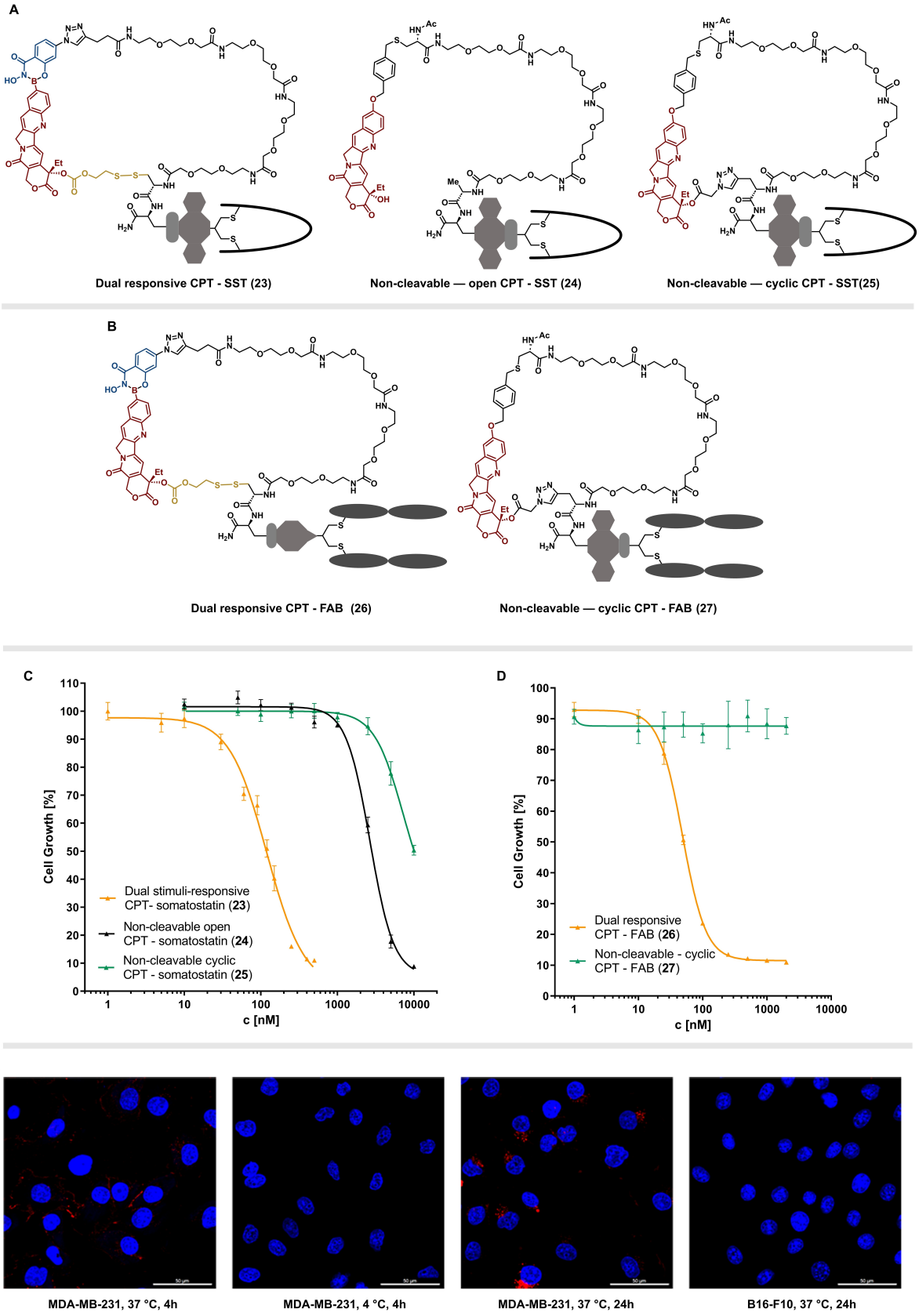

Figure 6. Structures of CPT derivatives conjugated to A) somatostatin and B) anti-EGFR, FAB fragment, which were subjected to proliferation assay of MDA-MB-231 cells. C) Determination of IC_{50} values for somatostatin conjugates using **23**, **24**, and **25**. D) Determination of IC_{50} values for FAB conjugates using **26** and **27**. E) Visualization of confocal laser scanning micrographs of MDA-MB-231 cells treated with 200 nM Alexa Fluor™ 594 labeled dual-responsive CPT–FAB, at 37 °C and 4 °C, for 4 h. MDA-MB-231 cells and B16-F10 cells treated with 200 nM Alexa Fluor™ 594 labeled dual-responsive CPT–FAB **26** for 24 h at 37 °C. Nucleus stained with Hoechst 33342 dye, scale bars: 50 μm.

the prepared CPT-SST derivatives **23**–**25** and determined their impact on cellular growth using Incucyte® over 110 h (Figure 6C). Dual-stimuli-responsive CPT-somatostatin construct **23** impeded cell growth in the cell proliferation assays (Figure 6C). Remarkably, the IC_{50} value was determined to be 119 ± 9 nM, which is in a similar range as 10-BA CPT (**6**, Figure 2C, IC_{50} 42.4 ± 1.1 nm). In clear contrast to this, non-cleavable cyclic CPT-somatostatin construct **25**, retaining its "closed" ring structure in the TME showed no cell growth inhibition in this concentration range (**25**, Figure 6C). Inhibitory effects were only observed starting at concentration of 5–10 μM (Figure 6C). The IC_{50} value was estimated to be in the order of 10 μM, being approximately 100 times higher than the dual-responsive analog. The non-cleavable open CPT **24**, which can be seen as an intermediate where one bond has already been cleaved, was more active than **25** (IC_{50} value 2.7 ± 0.1 μM), but still approximately 20-fold less potent than the dual-responsive derivative **23**, corroborating that both traceless stimuli are required to regenerate the efficient chemotherapeutic inside cells.

The epidermal growth factor receptor (EGFR) is highly expressed in different cancer types including MDA-MB-231, which was confirmed by western blot analysis (SI-Figure S70). Thus, we investigated the cellular uptake of the Fab-drug conjugate in MDA-MB-231 cells using Alexa Fluor™ 594 labeled dual responsive CPT-FAB (**26**, Figure 6E, Figures S59–S61 and S63), suggesting that the CPT-FAB conjugate penetrated into the EGFR-expressing MDA-MB-231 cells. The B16-F10 melanoma cell line, which is known to have a low expression of EGFR, [62] was used as a negative control to confirm receptor-mediated uptake of Alexa Fluor™ 594 labeled dual-responsive CPT-FAB **26** (Figure 6E, Figure S62). A clear difference in uptake of compound **26** was observed in the MDA-MB-231 cells compared to the B16-F10 cells after incubation for 4 h or 24 h incubation at 37 °C (Figure 6E). In addition, MDA-MB-231 cells was incubated with **26** for 4 h at 4 °C, where energy dependent internalization was quenched and no uptake was observed (Figure 6E). The results taken together confirmed the receptor-mediated uptake of the CPT-FAB construct. Next, the impact of attaching a bulky FAB to the cyclic CPT on the release and recovery was investigated. A proliferation assay of dual-responsive CPT-FAB **26** displayed high drug toxicity with an IC_{50} value of 48.4 ± 1.6 nM (Figure 6D), which was comparable to 10-BA CPT (**6**). On the other hand, non-cleavable-cyclic CPT-FAB **27** displayed no noticeable toxicity up to the tested maximum concentration of 5 μM. These results clearly demonstrate that only the dual-stimuli-responsive CPT conjugates **23** and **26** showed high cell toxicity comparable to the unmodified drug 10-BA CPT (**6**).

Notably, we demonstrated that conjugation of the macrocyclic CPT to biomacromolecules such as peptides and proteins had no detrimental effects on the toxicity of the released CPT (Figure 6C–D), further supporting traceless release. Our results clearly indicate that the dual-responsive cyclic locked drugs designed herein represent dual stimuli-controlled "turn-on" drugs for selective and traceless release, a versatile approach for improving the delivery of existing small-molecule therapeutics.

Conclusions

In this work, we demonstrated the potential of dynamic covalent chemistry to direct the macrocyclization of a small-molecule anticancer drug, CPT, to afford a locked, inactive prodrug in a cyclic form. Our strategy enables: 1) the incorporation of a targeting group that binds with high affinity to cell surface receptors; 2) the combination of two cross-orthogonal chemistries to direct cyclization in a stimuli-responsive manner; and 3) traceless release of free drug to its active form. Notably, the cyclic CPT showed lower binding to components in human serum and it was stable to cell components. We equipped the dual-locked cyclic CPT with two therapeutically relevant targeting entities: a cyclic peptide somatostatin that recognizes G-coupled protein receptor and an antibody protein fragment of Cetuximab (anti-EGFR, FAB fragment). Traceless release of the small molecules drug CPT from the cyclic drug conjugates took place under certain conditions mimicking intracellular space of cancer cells. Presumably, this enables the high recovery of CPT potency when the structure were unlocked within cancer cells. Overall, we have devised a new strategy for the convenient synthesis of dual stimuli responsive drugs through a cyclic locked, as well as enhanced the features of current repertoire of small-molecule therapeutics with the possibility for targeted delivery with controlled intracellular release. The dual-latch mechanism holds great promise to overcome the current limitations of existing systems, i.e., to prevent premature release of the active drug in the extracellular and often acidic TME or disulfide burst release during circulation in the bloodstream. Furthermore, by introducing a boronic acid into the design, we provide new chemical space for the innovation of medicinal drugs, which holds immense promise for the pharmaceutical development of safer and more efficient biotherapeutics.

Supporting Information

The Supporting Information gives the full experimental procedures, characterization data for new compounds, DFT calculations and in vitro studies.

Acknowledgements

We thank the Max Planck Society and the Deutsche Forschungsgemeinschaft (DFG, German Research Foundation) – project number 316249678 – SFB 1279 (C01) and project number 213555243 – SFB 1066 (Q05). L.N.C.R. acknowledges support from the EC (Project No. 859458), B.G. thanks the China Scholarship Council for her PhD scholarship. J.A.S.C. thanks the Fundação para a Ciência e a Tecnologia (FCT) for Scientific Employment Stimulus

2020/02383/CEECIND. We thank Sarah Chagri for the provision of compound **4** and its synthesis protocol and Dr. Joachim Räder for the HR-ESI-MS measurement of compound **11**. Open Access funding enabled and organized by Projekt DEAL.

Conflict of Interest

The authors declare no conflict of interest.

Data Availability Statement

The data that support the findings of this study are available from the corresponding author upon reasonable request.

Keywords: macrocyclic drugs · drug delivery · dual-responsive chemotherapeutics · traceless release

[1] Y.-S. Ma, J.-B. Liu, X.-L. Yang, R. Xin, Y. Shi, D.-D. Zhang, H.-M. Wang, P.-Y. Wang, Q.-L. Lin, W. Li, *Am. J. Cancer Res.* **2021**, *11*, 2386.
[2] P. Akkapeddi, S.-A. Azizi, A. M. Freedy, P. M. S. D. Cal, P. M. P. Gois, G. J. L. Bernardes, *Chem. Sci.* **2016**, *7*, 2954–2963.
[3] Z. Fu, S. Li, S. Han, C. Shi, Y. Zhang, *Signal Transduct. Target. Ther.* **2022**, *7*, 93.
[4] M. K. Greene, D. A. Richards, J. C. F. Nogueira, K. Campbell, P. Smyth, M. Fernández, C. J. Scott, V. Chudasama, *Chem. Sci.* **2018**, *9*, 79–87.
[5] A. Salvati, A. S. Pitek, M. P. Monopoli, K. Prapainop, F. B. Bombelli, D. R. Hristov, P. M. Kelly, C. Åberg, E. Mahon, K. A. Dawson, *Nat. Nanotechnol.* **2013**, *8*, 137–143.
[6] Z. Zhao, A. Ukidve, J. Kim, S. Mitragotri, *Cell* **2020**, *181*, 151–167.
[7] D. E. Large, J. R. Soucy, J. Hebert, D. T. Auguste, *Adv. Ther.* **2019**, *2*, 1800091.
[8] V. Estrella, T. Chen, M. Lloyd, J. Wojtkowiak, H. H. Cornnell, A. Ibrahim-Hashim, K. Bailey, Y. Balagurunathan, J. M. Rothberg, B. F. Sloane, *Cancer Res.* **2013**, *73*, 1524–1535.
[9] R. J. Gillies, Z. Liu, Z. Bhujwalla, *Am. J. Physiol.* **1994**, *267*, C195–C203.
[10] G. A. Robinson, R. W. Butcher, E. W. Sutherland, *Annu. Rev. Biochem.* **1968**, *37*, 149–174.
[11] J. J. Calvete, C. Marcinkiewicz, D. Monleón, V. Esteve, B. Celda, P. Juárez, L. Sanz, *Toxicon* **2005**, *45*, 1063–1074.
[12] A. A. Vinogradov, Y. Yin, H. Suga, *J. Am. Chem. Soc.* **2019**, *141*, 4167–4181.
[13] T. Passioura, T. Katoh, Y. Goto, H. Suga, *Annu. Rev. Biochem.* **2014**, *83*, 727–752.
[14] E. M. Driggers, S. P. Hale, J. Lee, N. K. Terrett, *Nat. Rev. Drug Discovery* **2008**, *7*, 608–624.
[15] M. J. McCall, H. Diril, C. F. Meares, *Bioconjugate Chem.* **1990**, *1*, 222–226.
[16] C. Lin, S. Maisonneuve, R. Métivier, J. Xie, *Chem. Eur. J.* **2017**, *23*, 14996–15001.
[17] M. M. Zegota, M. A. Müller, B. Lantzberg, G. Kizilsavas, J. A. S. Coelho, P. Moscariello, M. Martínez-Negro, S. Morsbach, P. M. P. Gois, M. Wagner, D. Y. W. Ng, S. L. Kuan, T. Weil, *J. Am. Chem. Soc.* **2021**, *143*, 17047–17058.
[18] J. Plescia, N. Moitessier, *Eur. J. Med. Chem.* **2020**, *195*, 112270.
[19] B. K. Agrawalla, T. Wang, A. Riegger, M. P. Domogalla, K. Steinbrink, T. Dörfler, X. Chen, F. Boldt, M. Lamla, J. Michaelis, S. L. Kuan, T. Weil, *Bioconjugate Chem.* **2018**, *29*, 29–34.
[20] M. Arzt, C. Seidler, D. Y. W. Ng, T. Weil, *Chem. Asian J.* **2014**, *9*, 1994–2003.
[21] M. Pieszka, S. Han, C. Volkmann, R. Graf, I. Lieberwirth, K. Landfester, D. Y. W. Ng, T. Weil, *J. Am. Chem. Soc.* **2020**, *142*, 15780–15789.
[22] S. Chagri, D. Y. W. Ng, T. Weil, *Nat. Chem. Rev.* **2022**, *6*, 320–338.
[23] M. P. Silva, L. Saraiva, M. Pinto, M. E. Sousa, *Molecules* **2020**, *25*, 4323.
[24] H. Sies, D. P. Jones, *Nat. Rev. Mol. Cell Biol.* **2020**, *21*, 363–383.
[25] S. P. Black, J. K. M. Sanders, A. R. Stefankiewicz, *Chem. Soc. Rev.* **2014**, *43*, 1861–1872.
[26] S. F. Betz, *Protein Sci.* **1993**, *2*, 1551–1558.
[27] A. Wilson, G. Gasparini, S. Matile, *Chem. Soc. Rev.* **2014**, *43*, 1948–1962.
[28] G. K. Balendiran, R. Dabur, D. Fraser, *Cell Biochem. Funct.* **2004**, *22*, 343–352.
[29] J. M. Estrela, A. Ortega, E. Obrador, *Crit. Rev. Clin. Lab. Sci.* **2006**, *43*, 143–181.
[30] X. Wang, X. Cai, J. Hu, N. Shao, F. Wang, Q. Zhang, J. Xiao, Y. Cheng, *J. Am. Chem. Soc.* **2013**, *135*, 9805–9810.
[31] D. M. Townsend, K. D. Tew, *Oncogene* **2003**, *22*, 7369–7375.
[32] D. Yang, W. Chen, J. Hu, *J. Phys. Chem. B* **2014**, *118*, 12311–12317.
[33] N. R. Ko, J. K. Oh, *Biomacromolecules* **2014**, *15*, 3180–3189.
[34] X. Chang, L. Liu, Y. Guan, C. Dong, *J. Polym. Sci. Part A* **2014**, *52*, 2000–2010.
[35] Q.-Y. Li, Y.-G. Zu, R.-Z. Shi, L.-P. Yao, *Curr. Med. Chem.* **2006**, *13*, 2021–2039.
[36] C. J. Thomas, N. J. Rahier, S. M. Hecht, *Bioorg. Med. Chem.* **2004**, *12*, 1585–1604.
[37] M. R. Redinbo, L. Stewart, P. Kuhn, J. J. Champoux, W. G. J. Hol, *Science* **1998**, *279*, 1504–1513.
[38] C. Tesauro, A. K. Simonsen, M. B. Andersen, K. W. Petersen, E. L. Kristoffersen, L. Algreen, N. Y. Hansen, A. B. Andersen, A. K. Jakobsen, M. Stougaard, *BMC Cancer* **2019**, *19*, 1–15.
[39] S. T. Liew, L.-X. Yang, *Curr. Pharm. Des.* **2008**, *14*, 1078–1097.
[40] M. E. Wall, *Med. Res. Rev.* **1998**, *18*, 299–314.
[41] F. Li, T. Jiang, Q. Li, X. Ling, *Am. J. Cancer Res.* **2017**, *7*, 2350.
[42] L. Wang, S. Xie, L. Ma, Y. Chen, W. Lu, *Eur. J. Med. Chem.* **2016**, *116*, 84–89.
[43] Z. Deng, J. Hu, S. Liu, *Macromol. Rapid Commun.* **2020**, *41*, 1900531.
[44] C. F. Riber, A. A. A. Smith, A. N. Zelikin, *Adv. Healthcare Mater.* **2015**, *4*, 1887–1890.
[45] Y. Ding, Y. Dai, M. Wu, L. Li, *Chem. Eng. J.* **2021**, *426*, 128880.
[46] G. Wu, Y.-Z. Fang, S. Yang, J. R. Lupton, N. D. Turner, *J. Nutr.* **2004**, *134*, 489–492.
[47] H. J. Forman, H. Zhang, A. Rinna, *Mol. Aspects Med.* **2009**, *30*, 1–12.
[48] P. T. Schumacker, *Cancer Cell* **2006**, *10*, 175–176.
[49] G.-Y. Liou, P. Storz, *Free Radical Res.* **2010**, *44*, 479–496.
[50] M. López-Lázaro, *Cancer Lett.* **2007**, *252*, 1–8.
[51] C. M. Doskey, V. Buranasudja, B. A. Wagner, J. G. Wilkes, J. Du, J. J. Cullen, G. R. Buettner, *Redox Biol.* **2016**, *10*, 274–284.
[52] Z. Chu, J. Yang, W. Zheng, J. Sun, W. Wang, H. Qian, *Coord. Chem. Rev.* **2023**, *481*, 215049.
[53] Z. Zhou, K. Maxeiner, P. Moscariello, S. Xiang, Y. Wu, Y. Ren, C. J. Whitfield, L. Xu, A. Kaltbeitzel, S. Han, *J. Am. Chem. Soc.* **2022**, *144*, 12219–12228.

[54] M. Burney, S. Mosley, A. O. Gonzalez, J. A. Smith, *Pharm. Pharmacol. Int. J.* **2017**, *4*, 98–102.
[55] D. Barton, O. Meth-Cohn, *Comprehensive Natural Products Chemistry*, Newnes, **1999**.
[56] R. M. Clegg, *Lab. Tech. Biochem. Mol. Biol.* **2009**, *33*, 1–57.
[57] Y. Hu, F. Zeng, *Mater. Sci. Eng. C* **2017**, *72*, 77–85.
[58] T. Wang, N. Zabarska, Y. Wu, M. Lamla, S. Fischer, K. Monczak, D. Y. W. Ng, S. Rau, T. Weil, *Chem. Commun.* **2015**, *51*, 12552–12555.
[59] E. Ragozin, A. Hesin, A. Bazylevich, H. Tuchinsky, A. Bovina, T. S. Zahavi, M. Oron-Herman, G. Kostenich, M. A. Firer, T. Rubinek, *Bioorg. Med. Chem.* **2018**, *26*, 3825–3836.
[60] J. Baselga, *Eur. J. Cancer* **2001**, *37*, 16–22.
[61] T. M. Brand, M. Iida, D. L. Wheeler, *Cancer Biol. Ther.* **2011**, *11*, 777–792.
[62] D. Jia, Y. Yang, F. Yuan, Q. Fan, F. Wang, Y. Huang, H. Song, P. Hu, R. Wang, G. Li, *Int. J. Pharm.* **2020**, *586*, 119541.

Manuscript received: September 21, 2023
Accepted manuscript online: January 5, 2024
Version of record online: March 27, 2024